SUPPORTING INFORMATION

Chinese Journal of Structural Chemistry

Spatially Isolated Noble-Metal-Free Redox Cocatalysts on CdS Nanorods for Increased Photocatalytic Hydrogen Generation

Xiaomeng Zhang[1+], Gege Zhao[1+], Zhongfei Li[1], Liang Zhu[1], Yingpeng Cheng[1], Haiwei Du[1], Chuhong Zhu[1], Ya Dang[3], Daochuan Jiang[1,3*] and Yupeng Yuan[1,2*]

[1]*School of Materials Science and Engineering, Anhui University, Hefei 230601, China*

[2]*Key Laboratory of Structure and Functional Regulation of Hybrid Materials (Anhui University), Ministry of Education, and Energy Materials and Devices Key Lab of Anhui Province for Photoelectric conversion, Anhui University, Hefei 230601, China*

[3]*Anhui Chinaherb Flavors & Fragrances Co., Ltd., Bengbu 233400, China*

**Corresponding author. Emails: jdczlx@ahu.edu.cn and yupengyuan@ahu.edu.cn*

n EXPERIMENTAL

Characterizations. The crystal structure was analyzed by the X-ray diffractometer (XRD) on a DX-2700 X-ray diffractometer with Cu Kα1 radiation (λ = 0.1541 nm). The morphology was observed by field-emission scanning electron microscopy (SEM, Regulus 8230) and transmission electron microscopy (TEM, JEM-2100). X-ray photoelectron spectra (XPS) were collected on an ESCALAB 250Xi instrument with Al Kα radiation. In-situ irradiation XPS (ISI-XPS) measurements were conducted under 500 and 700 nm visible light irradiation (AXIS SUPRA). Elemental analysis was performed on an elemental analyzer (Vario EL-3). The UV-vis diffuse reflectance spectra (DRS) were measured on a UV-vis spectrophotometer (HITACHI U-3900). Time-resolved photoluminescence (TR-PL) spectra were tested by a fluorescence spectrophotometer (HITACHI F-4500) and a spectrometer (Horiba Fluoro max plus), respectively. Single-particle photoluminescence (PL) images and spectra were recorded on an objective scanning confocal microscope system (PicoQuant, MicroTime 200) combined with an Olympus IX71 inverted fluorescence microscope. The excitation wavelength is 405 nm.

Photoelectrochemical Characterization. The electrochemical measurements, including electrochemical impedance spectra (EIS), transient photocurrent responses were conducted on an electrochemical workstation (Chenhua CHI-660E) in a standard three-electrode cell, in which the Ag/AgCl (saturated KCl), platinum (Pt) foil, and catalyst-coated fluorine-doped tin oxide (FTO) were used as the reference electrode, counter electrode, and working electrode, respectively. The Na_2S aqueous solution (0.75 M) and Na_2SO_3 aqueous solution (1.05 M) were used as the electrolyte in all electrochemical tests. The working electrode was prepared as follows: First, photocatalyst powder (5 mg) was dispersed in 0.5 mL mixed solution of Nafion and ethanol (1 mL Nafion (5 wt%) and 9 mL ethanol), respectively. Subsequently, the mixture was sonicated for 30 min to obtain a slurry, and then the slurry (50 μL) was drop-coated onto the FTO glass (coating area: 1 cm × 1 cm) and dried in air at room temperature before measurements.

Calculation of ECSA. The electrochemically active surface area (ECSA) of the electrocatalysts is evaluated by measurement of their double layer charging capacitance in 0.75 M 1.05 M Na_2S and Na_2SO_3 solution. Briefly, a potential range where no apparent Faradaic process occurred was determined firstly using cyclic voltammetry (CV). The charging current (i_c) in this potential range was then measured from CV plots at different scan rates. The relationship between i_c, the scan rate (v), and the double layer charging capacitance (C_{dl}) were governed by Eq. 1.

$$I_c = vC_{dl}$$

From the slope of the plot of i_c vs. v, C_{dl} could be obtained which is directly proportional to ECSA.

Photocatalytic Hydrogen Generation. The photocatalytic H_2 generation experiment was carried out in a 50 mL round bottom flask. Photocatalyst sample (5 mg) was first dispersed into a 20 mL Na_2S (0.25 M) and Na_2SO_3 (0.35 M) aqueous solution. Prior to photocatalytic reaction, the round bottom flask was sealed and then bubbled with Ar for 20 min to remove the residual air. Methane was used in the reactor as the internal standard. The photocatalytic H_2 generation was conducted under the irradiation of a 300 W Xe lamp with a 420 nm cut off filter, and the light intensity was measured to be 550 mW/cm^2 by a photometer. The H_2 thus generated was analyzed on a gas chromatograph instrument (GC-1690, Kexiao) with a thermal conductive detector (TCD), in which Ar was used as the carrying gas. The apparent quantum yield (AQY) was measured using a 300 W Xe-lamp equipped with a 420 nm bandpass cut filter. The AQY was calculated based on the following equation:

$$\text{AQY (\%)} = \frac{\text{number of of } H_2 \text{ molecules} \times 2}{\text{number of icident photons}} \times 100\%$$

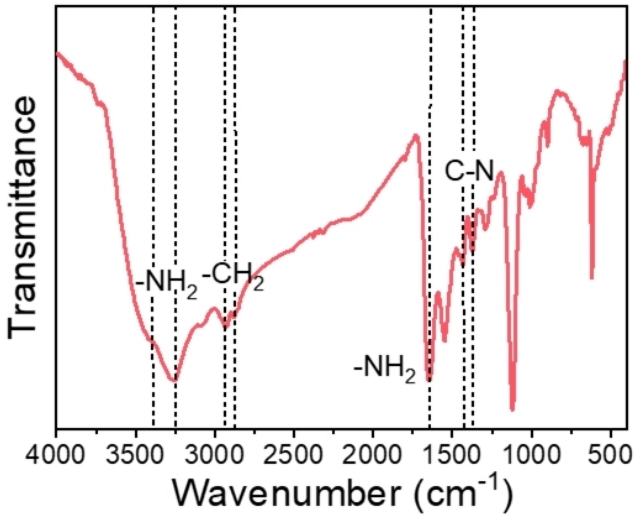

Figure S1. FT-IR spectrum of unpurified CdS nanorods.

Figure S1 is the FT-IR spectrum of unpurified CdS nanorods. It exhibits obvious EDA characteristic peaks. Specifically, the characteristic peaks of primary amine groups appeared at 3200~3400, 1500-1700, and 1300~1500 cm^{-1}, and the peak at 2750~2950 cm^{-1} for $-CH_2$ is also presented.[1]

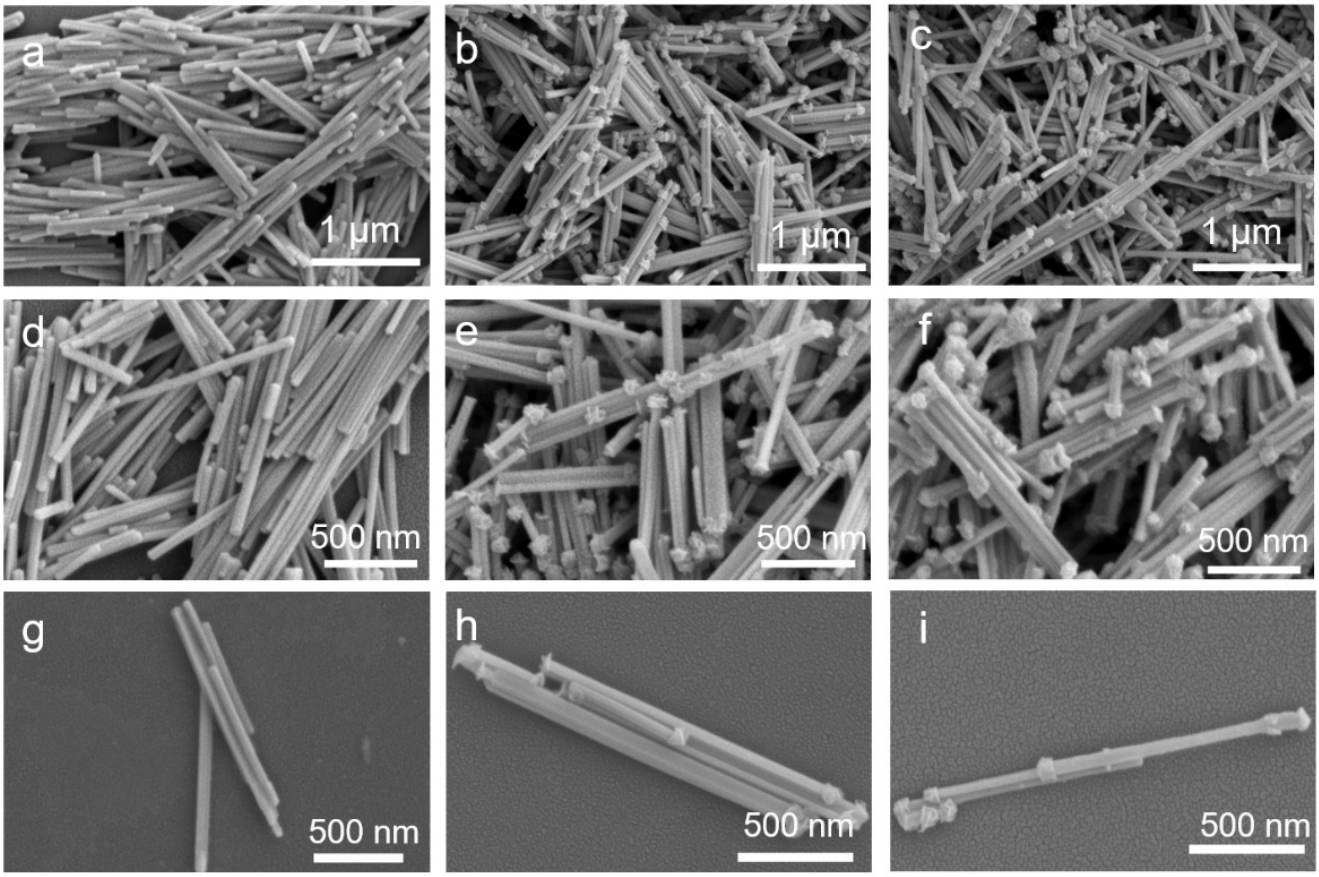

Figure S2. SEM images of pristine CdS (a), (d), (g), CdS/MoS_2 (b), (e), (h) and CdS/MoS_2/CoPi-5 (c), (f), (i).

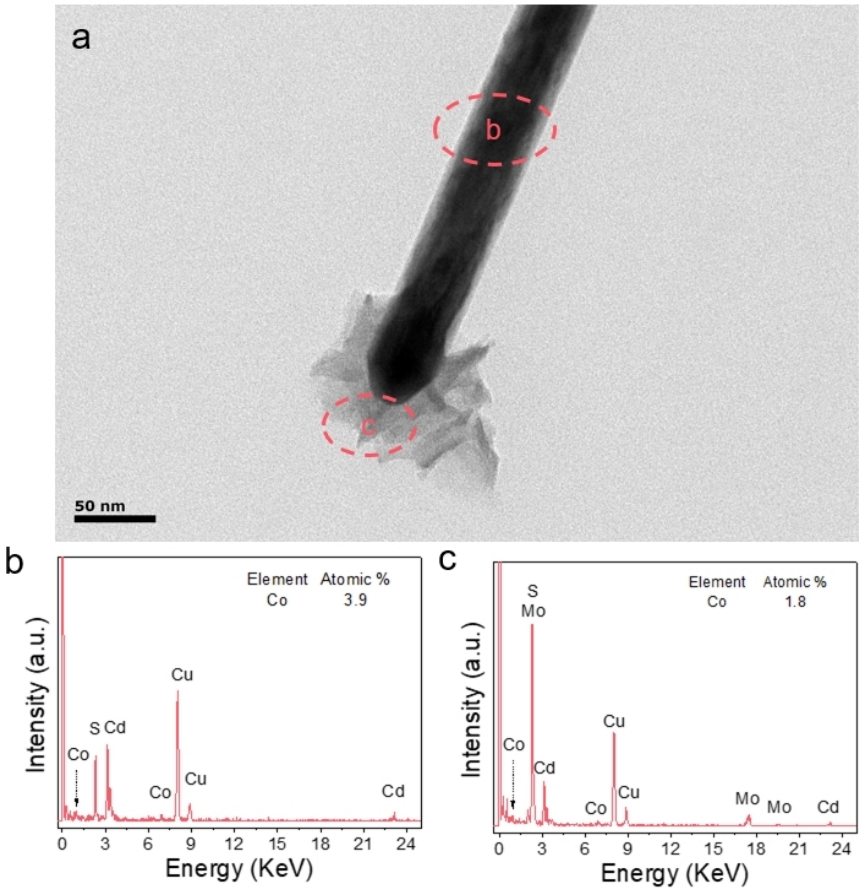

Figure S3. TEM image of an individual CdS/MoS_2/CoPi-5 nanorod (a). EDX spectra for the selected regions (b-c) in (a)

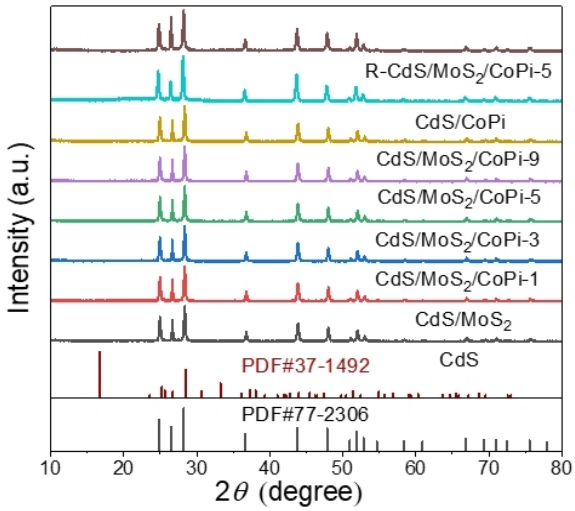

Figure S4. XRD patterns of CdS, CdS/MoS_2, CdS/MoS_2/CoPi-1, CdS/MoS_2/CoPi-3, CdS/MoS_2/CoPi-5, CdS/MoS_2/CoPi-9, CdS/CoPi, and R-CdS/MoS_2/CoPi-5 samples.

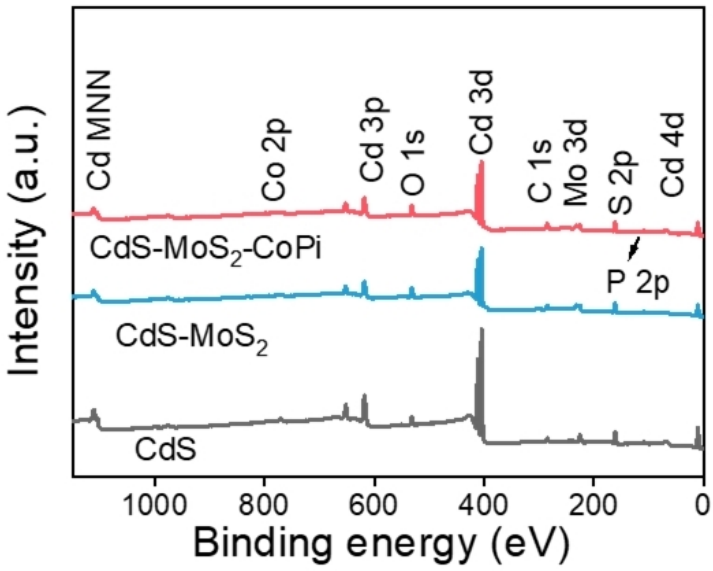

Figure S5. Survey spectra of pristine CdS, CdS/MoS_2, and CdS/MoS_2/CoPi-5.

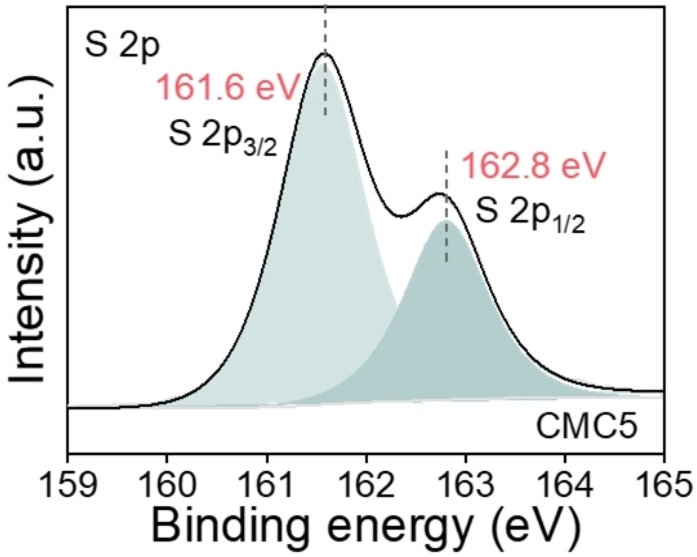

Figure S6. High-resolution XPS spectrum of S 2p in the CdS/MoS_2/CoPi-5 sample.

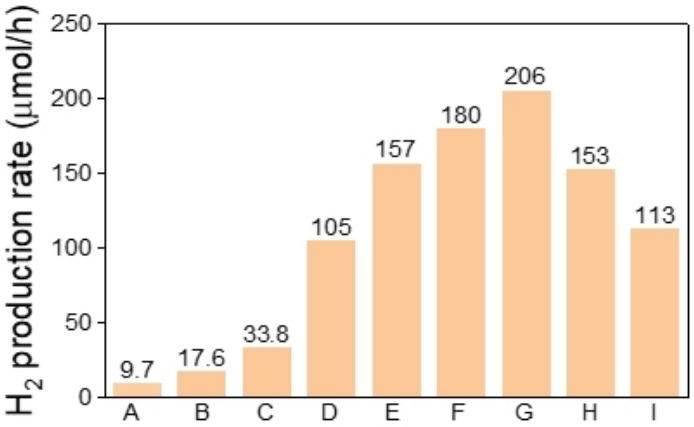

Figure S7. The H_2 production rate of different samples. (A) CdS, (B) CdS/CoPi, (C) CdS/Pt (D) CdS/MoS_2, (E) CdS/MoS_2/CoPi-1, (F) CdS/MoS_2/CoPi-3, (G) CdS/MoS_2/CoPi-5, (H) CdS/MoS_2/CoPi-9, (I) R-CdS/MoS_2/CoPi-5.

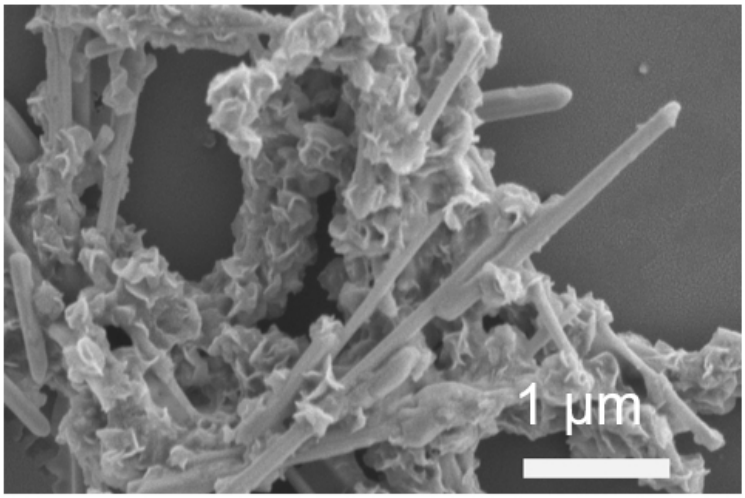

Figure S8. SEM image of the R-CdS/MoS_2/CoPi-5 sample.

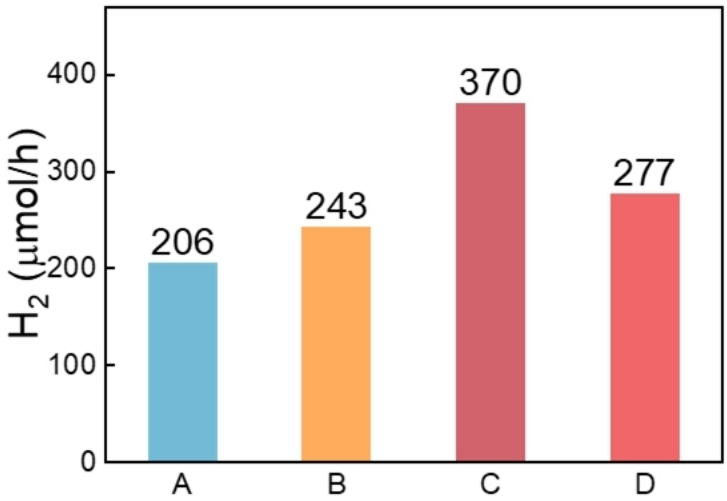

Figure S9. H_2 production rates of CdS/MoS_2/CoPi-5 in different concentrations of sacrificial reagents. (A) 0.25 M Na_2S, 0.35 M Na_2SO_3; (B) 0.50 M Na_2S, 0.70 M Na_2SO_3; (C) 0.75 M Na_2S, 1.05 M Na_2SO_3; (D) 1.0 M Na_2S, 1.4 M Na_2S

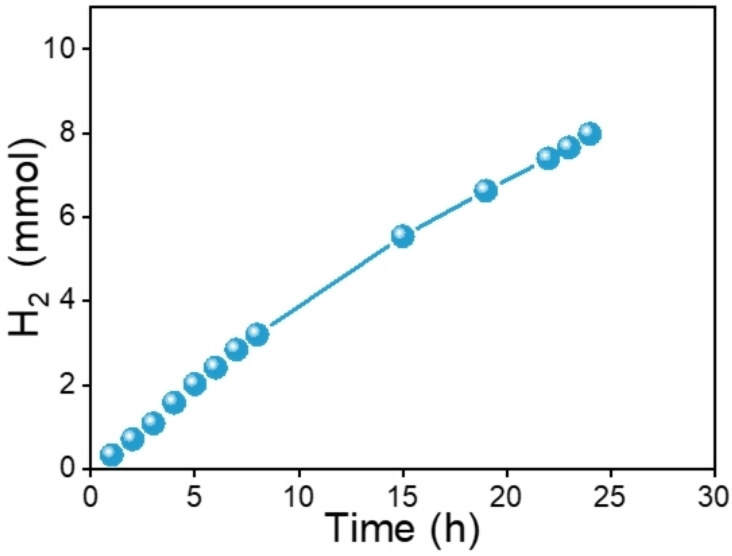

igure S10. The long-term stability tests of CdS/MoS_2/CoPi-5 sample for photocatalytic H_2 production.

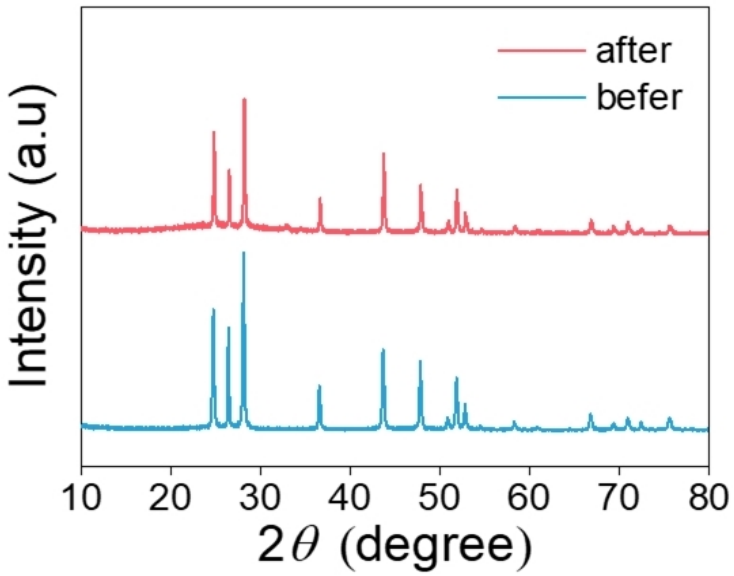

Figure S11. XRD patterns of CdS/MoS_2/CoPi-5 after irradiation.

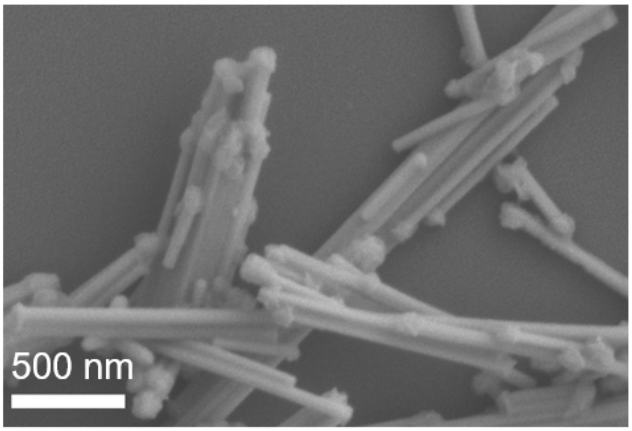

Figure S12. SEM image of CdS/MoS_2/CoPi-5 after irradiation.

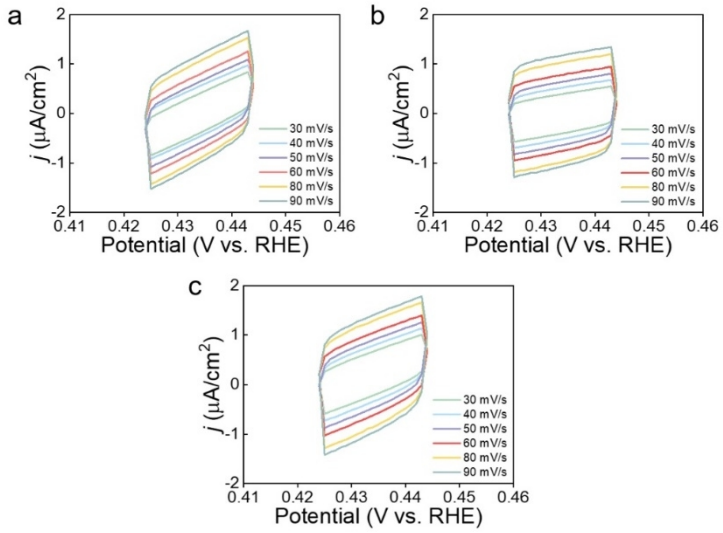

Figure S13. The double-layer capacitance (C_{dl}) measurements of (a), pristine CdS, (b), CdS/MoS_2, and (c), CdS/MoS_2/CoPi-5.

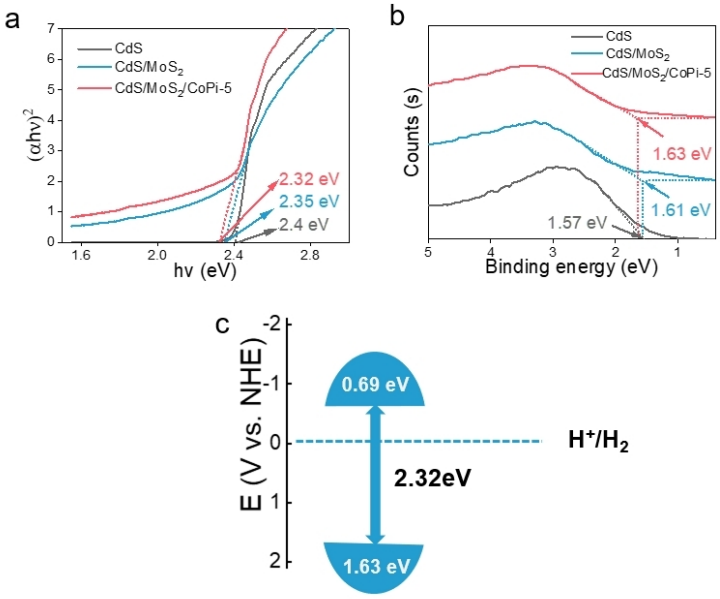

Figure S14. Tauc plots (a) and VB spectra (b) of CdS, CdS/MoS_2, and CdS/MoS_2/CoPi-5. (c) Energy level diagram of CdS/MoS_2/CoPi-5.

As shown in Figure S14a, the Tauc plots demonstrate that the band gaps of CdS, CdS/MoS_2 and CdS/MoS_2/CoPi-5 are 2.4, 2.35, and 2.32 eV, respectively. In addition, the valence band edge positions of CdS, CdS/MoS_2, and CdS/MoS_2/CoPi-5 obtained by the XPS valence band spectra are determined to be 1.57, 1.61, and 1.63 eV, respectively. The energy level diagram of CdS/MoS_2/CoPi-5 is thus obtained (Figure S14c).

Table S1. Comparison with Some Recently Reported CdS-Based Ternary Photocatalysts in Literatures for H_2 Production

Photocatalyst	Light source	Sacrificial reagent	H_2 generation rate [μmol $h^{-1}g^{-1}$]	AQY [%]	Ref. [year]
CdS/MoS_2/CoPi	300 W Xe lamp λ > 420 nm	1.05 M Na_2S 0.75 M Na_2SO_3	74000	30.9 (420 nm)	This work
CdS/Ag_2S/NiS	300 W Xe lamp λ > 420 nm	10 vol.% lactic acid	48280	49.5 (420 nm)	2021[2]
Pd/CdS/PdS	300 W Xe lamp λ > 400 nm	0.5 M Na_2S 0.5 M Na_2SO_3	144800	/	2018[3]
CdS/Au/Pt	300 W Xe lamp λ > 400 nm	0.25 M Na_2S 0.35 M Na_2SO_3	778	/	2016[4]
CdS/MoS_2/CoPi	300 W Xe lamp λ > 420 nm	10 vol.% lactic acid	40500	/	2019[5]
CdS/MoS_2/CoO_x	300 W Xe lamp	15% TEOA	7400	7.6 (420 nm)	2022[6]
CdS/Co/MoS_x	300 W Xe lamp λ＞420 nm	10 vol% lactic acid	12500	23.5 (420 nm)	2017[7]
CdS/MnOx/CuS	300W Xe lamp (420–780nm)	0.1 M Na2S 0.1 M Na2SO3	2400	4.89 (365 nm)	2019[8]
CdS/RGO/g-C3N4	350 W Xe lamp (400 < λ < 800 nm)	10 vol% lactic acid	676.5	36.5 (400<λ<800 nm)	2017[9]
NiS/CDs/CdS	350 W Xe lamp, λ > 420 nm	0.25 M Na_2S 0.35 M Na_2SO_3	1444	/	2018[10]

n REFERENCES

(1) Hu, J.; Xie, J.; Jia, W.; Zhang, S.; Wang, S.; Wang, K.; Cao, Y. Interesting molecule adsorption strategy induced energy band tuning: boosts 43 times photocatalytic water splitting ability for commercial TiO_2. *Appl. Catal. B-Environ.* **2020**, 268, 118753.

(2) He, B.; Bie, C.; Fei, X.; Cheng, B.; Yu, J.; Ho, W.; Al-Ghamdi, A. A.; Wageh, S. Enhancement in the photocatalytic H_2 production activity of CdS NRs by Ag_2S and NiS dual cocatalysts. *Appl. Catal. B-Environ.* **2021**, 288, 119994.

(3) Sun, Q.; Wang, N.; Yu, J.; Yu, J. C. A hollow porous CdS photocatalyst. *Adv. Mater.* **2018**, 30, 1804368.

(4) Ma, L.; Chen, K.; Nan, F.; Wang, J.-H.; Yang, D.-J.; Zhou, L.; Wang, Q.-Q. Improved hydrogen production of Au-Pt-CdS hetero-nanostructures by efficient plasmon-induced multipathway electron transfer. *Adv. Funct. Mater.* **2016**, 26, 6076-6083.

(5) Lu, K.-Q.; Qi, M.-Y.; Tang, Z.-R.; Xu, Y.-J. Earth-abundant MoS_2 and cobalt phosphate dual cocatalysts on 1D CdS nanowires for boosting photocatalytic hydrogen production. *Langmuir* **2019**, 35, 11056-11065.

(6) Di, T.; Deng, Q.; Wang, G.; Wang, S.; Wang, L.; Ma, Y. Photodeposition of CoO_x and MoS_2 on CdS as dual cocatalysts for photocatalytic H_2 production. *J. Mater. Sci. Technol.* **2022**, 124, 209-216.

(7) Lei, Y.; Hou, J.; Wang, F.; Ma, X.; Jin, Z.; Xu, J.; Min, S. Boosting the catalytic performance of MoS_x cocatalysts over CdS nanoparticles for photocatalytic H_2 evolution by Co doping via a facile photochemical route. *Appl. Surf. Sci.* **2017**, 420, 456-464.

(8) Zhao, F.; Li, H.; Liu, T.; Wang, Y. Spatially separated CdS hollow spheres with interfacial charge transfer and cocatalyst for enhancing photocatalytic hydrogen evolution. *Mol. Catal.* **2019**, 474, 110418.

(9) Jo, W.-K.; Selvam, N. C. S. Z-scheme CdS/g-C3N4 composites with RGO as an electron mediator for efficient photocatalytic H_2 production and pollutant degradation. *Chem. Eng. J.* **2017**, 317, 913-924.

(10) Wei, R.-B.; Huang, Z.-L.; Gu, G.-H.; Wang, Z.; Zeng, L.; Chen, Y.; Liu, Z.-Q. Dual-cocatalysts decorated rimous CdS spheres advancing highly-efficient visible-light photocatalytic hydrogen production. *Appl. Catal. B-Environ.* **2018**, 231, 101-107.